

# Quantum simulation of general semi-classical Rabi model beyond strong driving regime

Kunzhe Dai,<sup>1, a)</sup> Haiteng Wu,<sup>1, a)</sup> Peng Zhao,<sup>1</sup> Mengmeng Li,<sup>1</sup> Qiang Liu,<sup>1</sup> Guangming Xue,<sup>2</sup> Xinsheng Tan,<sup>1, b)</sup> Haifeng Yu,<sup>1, 2, c)</sup> and Yang Yu<sup>1, 2</sup>

<sup>1)</sup>*National Laboratory of Solid State Microstructures, School of Physics, Nanjing University, Nanjing 210093, China*

<sup>2)</sup>*Synergetic Innovation Center of Quantum Information & Quantum Physics, University of Science and Technology of China, Hefei, Anhui 230026, China*

(Dated: 2 October 2017)

We propose a scheme to simulate the interaction between a two-level system and a classical light field. Under the transversal driving of two microwave tones, the system Hamiltonian is identical to that of the general semi-classical Rabi model. We experimentally realize this Hamiltonian with a superconducting transmon qubit. By tuning the strength, phase and frequency of the two microwave driving fields, we simulate the quantum dynamics from weak to extremely strong driving regime. The resulting evolutions gradually deviate from the normal sinusoidal Rabi oscillations with increasing driving strength, in accordance with the predictions of the general semi-classical Rabi model far beyond the weak driving limit. Our scheme provides an effective approach to investigate the extremely strong interaction between a two-level system and a classical light field. Such strong interactions are usually inaccessible in experiments.

PACS numbers: 85.25.Cp, 42.50.Ct, 42.50.Hz

Light-matter interaction has been at the heart of important modern discoveries of fundamental effects, both classical and quantum mechanical<sup>1</sup>. As the simplest form of light-matter interaction, a two-level atom interacting with a classical light field, which was introduced by I. I. Rabi<sup>2</sup>, has been actively investigated to study and control various quantum systems, including that of nuclear magnetic resonance<sup>3</sup>, cavity quantum electrodynamics (QED)<sup>4</sup>, and circuit QED<sup>5,6</sup>. Based on this semi-classical model<sup>7</sup>, Jaynes and Cummings introduced a fully quantized version, i.e. quantum Rabi model<sup>8,9</sup>, which describes a two-level atom interacting with a quantum field mode. This model is a cornerstone of various areas of quantum physics such as quantum optics and quantum information processing.

As per the usual description of the Rabi model (semi-classical or quantum), the interaction between the atom and the field mode (classical or quantum) can be decomposed into two parts, i.e. the rotating and the counter-rotating terms. Usually, the coupling is significantly smaller than the atomic transition frequency and field mode frequency. In this weak-coupling regime, the dynamics of the atom-field system is well described by the Rabi model with the usual rotating wave approximation (RWA)<sup>8,9</sup>, i.e. omitting the counter-rotating terms. However, when the coupling is comparable to the atomic transition frequency and field mode frequency, a limit which can be dubbed ultrastrong coupling (USC) regime, the usual RWA breaks down<sup>10</sup>, consequently the counter-rotating terms manifest important impact on the dynam-

ics of the atom-field system<sup>11–13</sup>. Xie *et al.*<sup>14</sup> have introduced an anisotropic version of the quantum Rabi model thus generalized the quantum Rabi model to USC regime. The experimental explorations of light-matter interaction in ultra-strong coupling regime has long been restricted by the coupling strength between the atom and field. Recently, a few experiments have reached USC regime in solid state system<sup>15–25</sup> and have demonstrated complex dynamics unique to this regime, e.g. the Bloch-Siegert shift<sup>18,19</sup>, the Floquet state<sup>20</sup>, exotic behaviors distinct from the normal sinusoidal Rabi oscillation<sup>15–17</sup>, and the spectroscopic signatures of these driving regimes<sup>21–25</sup>. However, it still remains an interesting but tough object to achieve driving strength that is significantly larger than the atomic transition frequency and field mode frequency (deep coupling regime<sup>26</sup>). As an alternative to access this fascinating field, quantum simulation of light-matter interaction in deep strong coupling (for quantum Rabi model) or extremely strong driving (for semi-classical Rabi model) would be helpful for researching and/or understanding various associated effects<sup>27–33</sup>.

In this paper, first we propose a scheme to simulate the general semi-classical Rabi model, for which the rotating and counter-rotating terms have two different driving strengths. By using bichromatic driving, we can engineer the desired effective Hamiltonian describing the generalized semi-classical Rabi model in various driving regimes. Then we experimentally realize the effective Hamiltonian in a circuit-QED setup, where a superconducting transmon qubit is driven by two phase-locked microwave tones simultaneously. We observe the dynamics of this light-matter interaction system in different driving regimes. The population evolutions gradually deviate from the normal sinusoidal Rabi oscillations with increasing driving strength. From weak to extremely strong driving

<sup>a)</sup>These authors contributed equally to this work

<sup>b)</sup>Electronic mail: txs.nju@gmail.com

<sup>c)</sup>Electronic mail: hfyu@nju.edu.cn

regimes, the system's behavior can be well described by the general semi-classical Rabi model. Our scheme thus provides an effective approach to explore the extremely strong interaction between a two-level system and a classical light field, such strong interaction is usually inaccessible in experiments.

The Hamiltonian of the generalized semi-classical Rabi model is given as<sup>14</sup>

$$\begin{aligned}\hat{H}/\hbar &= \frac{\omega_a}{2}\hat{\sigma}_z + A_d(H_r + \lambda H_{cr}), \\ \hat{H}_r/\hbar &= e^{i\omega_a t}\hat{\sigma}_- + e^{-i\omega_a t}\hat{\sigma}_+, \\ \hat{H}_{cr}/\hbar &= e^{-i\omega_a t}\hat{\sigma}_- + e^{i\omega_a t}\hat{\sigma}_+.\end{aligned}\quad (1)$$

where  $\hat{\sigma}_z$  is the Pauli matrices,  $\hat{\sigma}_-$  ( $\hat{\sigma}_+$ ) are the ladder operators for the atom of frequency  $\omega_a$ ,  $A_d$  is the driving strength of the rotating interaction  $\hat{H}_r$ , and  $\lambda$  is the relative strength between the rotating terms  $\hat{H}_{cr}$  and counter-rotating terms  $\hat{H}_r$ . When  $\lambda = 1$ , the Hamiltonian reduces to that of the usual semi-classical Rabi model. When  $\lambda \neq 1$ , this generalization can be considered as a semi-classical version of the anisotropic Rabi model<sup>14</sup>, or as the anisotropic generalization of the semi-classical Rabi model.

In order to reach the strong driving regime, we employ a bichromatic driving, rather than a single large amplitude<sup>20</sup>, to drive the two-level system. The Hamiltonian under the bichromatic driving in the laboratory frame with RWA can be written as

$$\begin{aligned}\hat{H}/\hbar &= \frac{\omega_a}{2}\hat{\sigma}_z + \frac{\Omega_1}{2}(e^{+i(\omega_1 t + \varphi_1)}\hat{\sigma}_- + \text{H.c.}) \\ &+ \frac{\Omega_2}{2}(e^{+i(\omega_2 t + \varphi_2)}\hat{\sigma}_- + \text{H.c.}).\end{aligned}\quad (2)$$

with  $\Omega_i$  the driving strength and  $\omega_i$  the frequency of the  $i$  (1,2)th drive.  $\varphi_i$  denotes the relative phase of the  $i$ th driving in the coordinate system of the qubit Bloch sphere in the laboratory frame.

Then we transform from the laboratory frame to a reference frame that rotates about the  $z$  axis using the unitary transformation,  $U_1 = \exp[-i\omega t\sigma_z/2]$ , with  $\omega = (\omega_1 + \omega_2)/2$ . Finally we apply a time-independent rotation,  $U_2 = \exp[-i\phi\sigma_z/2]$ , with  $\phi = (\varphi_1 + \varphi_2)/2$ . Since  $H_{\text{eff}} = U^{-1}HU - iU^{-1}\dot{U}$ , after the above two steps the original Hamiltonian in Eq. (2) becomes,

$$\begin{aligned}\hat{H}_{\text{eff}}/\hbar &= \frac{\omega_a^*}{2}\hat{\sigma}_z + \frac{\Omega_1}{2}(e^{+i(\omega_d^* t + \varphi_0^*)}\hat{\sigma}_- + \text{H.c.}) \\ &+ \frac{\Omega_2}{2}(e^{-i(\omega_d^* t + \varphi_0^*)}\hat{\sigma}_- + \text{H.c.}).\end{aligned}\quad (3)$$

Here we find that the effective qubit energy splitting  $\omega_a^* \equiv \omega_a - \omega$ , the effective light field frequency  $\omega_d^* \equiv \frac{1}{2}(\omega_1 - \omega_2)$ ,  $\omega_1 > \omega_2$ , and the initial phase  $\varphi_0^* = (\varphi_1 - \varphi_2)/2$ . The driving regime is now completely determined by the tunable parameters  $\omega_a^*$ ,  $\omega_d^*$ ,  $\Omega_1$ , and  $\Omega_2$ . Under the condition  $\Omega_1 = \Omega_2 = \Omega^*$ , the effective Hamiltonian can be reduced to

$$\hat{H}_{\text{eff}}/\hbar = \frac{\omega_a^*}{2}\hat{\sigma}_z + \Omega^* \cos(\omega_d^* t + \varphi_0^*)\sigma_x.\quad (4)$$

Eq. (4) is identical to the semi-classical Rabi Hamiltonian. It is interesting to observe the close resemblance between the formalism of the effective Hamiltonian in Eq. (3) and that of the Hamiltonian given in Eq. (1). This implies that we can simulate the generalized semi-classical Rabi model with controllable parameters. For a qubit with fixed  $\omega_a$ , we can tune  $\omega$  and  $\Omega_{1,2}$ , thus changing the system from weak driving, to ultrastrong driving  $\Omega_{1,2} > 0.1\omega_a^*$ , then deep strong driving  $\Omega_{1,2} > \omega_a^*$ , and even extremely strong driving  $\Omega_{1,2} \gg \omega_a^*$ . By choosing different parameters, we can investigate the behaviors in anisotropic Rabi model, phase sensitivity, and bias-modulated dynamics<sup>34-36</sup> in various driving regimes.

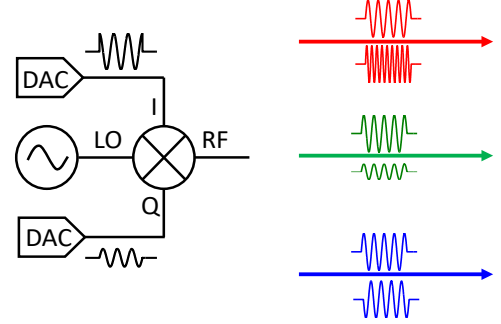


FIG. 1. (Color Online) The schematic of the bichromatic driving scheme, capable of generating two distinct microwave tones, each with its own tunable frequency, strength, and phase, as illustrated by different colors in the figure.

We use a 3D transmon qubit to experimentally implement the quantum simulation. A 3D transmon qubit comprises a superconducting transmon qubit and an aluminum holder in which the qubit sits, forming a typical circuit QED system. By our design, the detuning between the qubit frequency and cavity frequency is much larger than the coupling strength between the qubit and the cavity, thus the system works in the dispersive region. The main purpose of the cavity in our experiments is to serve as a convenient tool to manipulate and measure the qubit. The sample is cooled in a cryogen-free dilution refrigerator to a base temperature of about 20 mK. The details of qubit control and measurement can be found elsewhere<sup>37</sup>. From spectroscopy measurement, we obtain the qubit transition frequency at  $\sim 7.173$  GHz, the frequency difference between the ground state and the first excited state of the qubit. The resonant frequency of the 3D cavity is  $\sim 9.052$  GHz. The coupling strength between the qubit and the cavity is about 50 MHz. The energy relaxation time of the qubit is about 10  $\mu$ s and the decoherence time measured from Ramsey experiment is about 10  $\mu$ s.

In order to ensure phase control of the driving microwaves with respect to the qubit Bloch sphere coordinate system, we use a single microwave source together

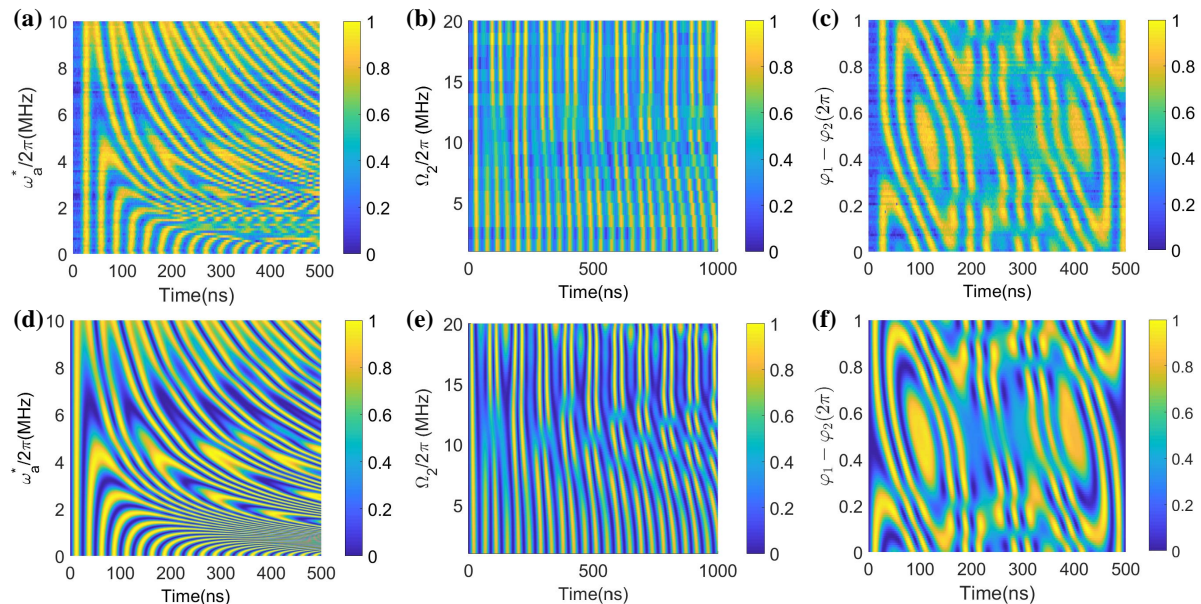


FIG. 2. (Color Online) Qubit evolution in strong driving regime. (a), (b), and (c) are measured qubit population as a function of time for tuning different parameters. (d), (e), and (f) are the corresponding numerical simulations with Hamiltonian in Eq. (3).

with two digital to analog converter(DAC) channels of an Arbitrary Wave Generator(AWG) of the model Tektronix 5014c to generate two microwave tones. Our bichromatic driving scheme (shown in Fig. 1) is different from that typical used in strong driving experiments<sup>33</sup>. We use only one microwave source for Local Oscillator(LO) input, with frequency equal to the mean frequency of the two tones and amplitude fixed. The two DAC channels synchronously generate a cosine and a sine waveform of different amplitudes for heterodyne IQ (In-phase and Quadrature) mixing. Except for the difference of a quadrature, these two waveforms have the same frequency and initial phase. Using this scheme, we can obtain two separate microwave tones with fully controllable frequency, strength and phase, which have simple relations to the input waveforms and can be readily deduced. The power of microwave required in this experiment is less than 20 dBm (corresponding to driving strength at  $2\pi \times 50$  MHz under our experimental setup), and the frequency applied is comparable to qubit transition frequency. These requirements are met by most microwave sources from common brands.

Setting	$\omega_1 - \omega_a$	$\omega_2 - \omega_a$	$\Omega_1$	$\Omega_2$	$\varphi_1 - \varphi_2$	$\omega_a^*$	$\omega_d^*$	$\varphi_0^*$
a	0	0~20	20	20	0	0~10	0~10	0
b	0	10	20	1~20	0	5	5	0
c	0	10	20	20	0~ $2\pi$	5	5	0~ $\pi$

TABLE I. The parameters used for quantum simulations in strong driving regime. The frequency and the driving strength are in the unit of  $2\pi$  MHz, while the phase in radians. We used the same parameters for numerical simulations.

According to Eq. (3), we can individually tune multiple parameters to simulate quantum dynamics in strong driving regime. In our experiments, we choose three representative settings to fulfill the requirement of strong driving. Table I lists the parameters used for different settings. At first, we keep the driving strength constant, i.e.  $\Omega_1/2\pi = \Omega_2/2\pi = 20$  MHz, the model reduces to Rabi model as described in Eq. (4). The initial phases of both microwave tones are the same, rendering  $\varphi^* = 0$ . As we keep the first microwave tone in resonance with the qubit and change the frequency of the second tone, we obtain different values for the effective transition frequency  $\omega_a^*$ , hence also for the ratio  $\Omega^*/\omega_a^*$ , which scales the relative driving strength. Shown in Fig. 2(a) is the qubit population at the first excited state as a function of time for different driving strengths with  $\omega_a^*/2\pi$  adjusted from 10 MHz to 0, corresponding to the ratio  $\Omega^*/\omega_a^*$  increasing from 2 to infinity. The system in the process reaches and even goes beyond the deep strong driving regime. The resulting oscillations are obviously anharmonic and nonlinear, exhibiting the dynamics of semi-classical Rabi model. In the second setting, we only change the driving strength of the second microwave tone  $\Omega_2$  and keep the other parameters fixed. From Eq. (3) we can see that  $\Omega_2$  defines the strength of the counter rotating field. This setting can be used to investigate the anisotropic Rabi model. We measure the qubit population evolution under various values for  $\Omega_2$ , as shown in Fig. 2(b). When  $\Omega_2$  is small, corresponding to the bottom part of Fig. 2(b), distinctly sinusoidal oscillations are observed because the effects of the counter-rotating terms are negligible. With the increase of  $\Omega_2$ , the sinusoidal fringes deform

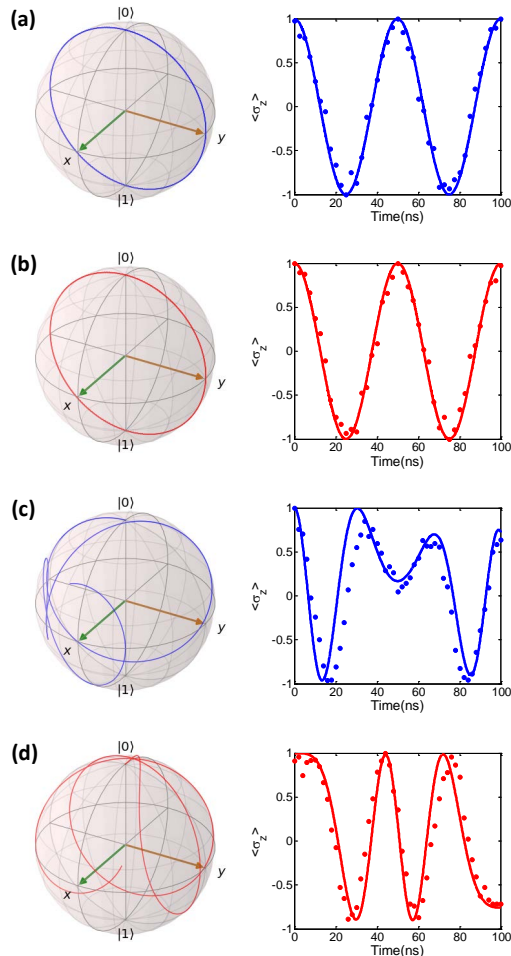


FIG. 3. (Color Online) The time evolution dynamics in Bloch sphere representation (left) and the corresponding  $\langle \sigma_z \rangle$  component (right) of the state vector with different initial phases. (a) and (b) [(c) and (d)] are evolutions in weak (deep strong) driving limit, with initial phase  $\varphi_0^* = 0$  and  $\pi/2$ , respectively. Solid lines and symbols correspond to theoretical calculation and experimental data.

and transition into an irregular pattern, exhibiting the influence of the counter-rotating terms under large  $\Omega_2$ . In the third setting, we only change the phase difference of the two tones, which defines the initial phase  $\varphi^*$  in the effective Hamiltonian in Eq. (3). In the weak driving regime this initial phase has negligible effects on the dynamics of the system<sup>17,38</sup>. However, this is not the case when we set the parameters for strong driving regime and measure the corresponding qubit evolution, as shown in Fig. 2(c), in which the phase-sensitivity of the evolution dynamics is evident. We note that the period of phase  $\varphi_0^*$  for this pattern is  $\pi$  instead of  $2\pi$ . In addition, we provide numerical simulation results by solving the master equations. The computed qubit evolutions agree with the experimental results.

In strong driving regime, a remarkable feature is the presence of counter-rotating evolution, which interestingly shows the initial phase dependence<sup>16,38</sup>. One of the advantages of our scheme is precise control of initial phase. As a result, we can investigate the dynamics with a specific initial phase instead of using an averaged phase<sup>16,38</sup>. Fig. 3 shows the state evolution on Bloch sphere (left) and its corresponding  $\langle \sigma_z \rangle$  component (right) as a function of time. For simplicity, we choose on-resonance condition  $\omega_d^* = \omega_a^*$ . By changing the values of  $\omega_a^*$  while keeping  $\Omega^*/2\pi = 20$  MHz, we simulate the dynamics from weak driving to deep strong driving regime. For (a) [(c)] and (b) [(d)],  $\varphi_0^* = 0$  and  $\pi/2$ , respectively. In Fig. 3(a), (b),  $\omega_a^*/2\pi = 2$  GHz, which is much larger than  $\Omega^*/2\pi$ . The system is in weak driving regime, where RWA is valid. The qubit state vector rotates normally in the  $y$ - $z$  plane on the surface of the Bloch sphere and the trajectories of both  $\varphi_0^*$ 's coincide. In Fig. 3(c), (d),  $\omega_a^*/2\pi = 5$  MHz, and  $\Omega^* > \omega_a^*$ , corresponding to the deep strong driving regime. Two trajectories completely deviate from the  $y$ - $z$  plane, the  $\langle \sigma_z \rangle$  component of state vector shows complicated oscillations. The trajectories of state vector for two initial phases are completely different. The dynamics exhibits strong sensitivity to initial phase. These phenomena result from the significant contribution of counter-rotating terms. In addition, the oscillations of  $\langle \sigma_z \rangle$  component agree with the numerical simulations, indicating precise control of the initial phase realized by our scheme.

In summary, we propose a bichromatic driving method to simulate the general Rabi model in strong driving regime. This method allows us to reach the strong driving regime with easily attainable experimental conditions. We demonstrate the dynamics of general Rabi model in various driving regimes. When the driving strength is higher than the effective energy splitting  $\omega_a^*$ , the model exhibits highly anharmonic and nonlinear behaviors, clearly deviating from the usual sinusoidal Rabi oscillations. Such effects manifest the influence of the counter-rotating terms upon the breakdown of RWA. Moreover, these sophisticated patterns and trajectories, obtained experimentally, are in agreement with the computed results. This quantum simulation scheme provides a useful test bed for studying general Rabi model in regimes defined by arbitrarily strong driving, and for exploring optimal quantum gate operations.

This work was partly supported by the the NKRD of China (Grant No. 2016YFA0301802), NSFC (Grant No. 11504165, No. 11474152, No. 61521001).

<sup>1</sup>C. Cohen-Tannoudji, J. Dupont-Roc, G. Grynberg, and P. Thickstun, *Atom-photon interactions: basic processes and applications* (Wiley Online Library, 1992).

<sup>2</sup>I. I. Rabi, Phys. Rev. **51**, 652 (1937).

<sup>3</sup>L. M. K. Vandersypen and I. L. Chuang, Rev. Mod. Phys. **76**, 1037 (2005).

<sup>4</sup>S. Haroche and J. M. Raimond, *Exploring the quantum: atoms, cavities, and photons* (Oxford university press, 2006).

<sup>5</sup>A. Blais, J. Gambetta, A. Wallraff, D. I. Schuster, S. M. Girvin,

- M. H. Devoret, and R. J. Schoelkopf, *Phys. Rev. A* **75**, 032329 (2007).
- <sup>6</sup>J. Q. You and F. Nori, *Phys. Rev. B* **68**, 064509 (2003).
- <sup>7</sup>D. Braak, Q. H. Chen, M. T. Batchelor, and E. Solano, *J. Phys. A: Math. Theor.* **49**, 300301 (2016).
- <sup>8</sup>E. T. Jaynes and F. W. Cummings, *Proc. IEEE* **51**, 89 (1963).
- <sup>9</sup>M. Tavis and F. W. Cummings, *Phys. Rev.* **170**, 379 (1968).
- <sup>10</sup>F. Bloch and A. Siegert, *Phys. Rev.* **57**, 522 (1940).
- <sup>11</sup>X. Cao, J. Q. You, H. Zheng, and F. Nori, *New J. Phys.* **13**, 073002 (2011).
- <sup>12</sup>S. Ashhab and F. Nori, *Phys. Rev. A* **81**, 042311 (2010).
- <sup>13</sup>D. Zueco, G. M. Reuther, S. Kohler, and P. Hänggi, *Phys. Rev. A* **80**, 033846 (2009).
- <sup>14</sup>Q. T. Xie, S. Cui, J. P. Cao, L. Amico, and H. Fan, *Phys. Rev. X* **4**, 021046 (2014).
- <sup>15</sup>G. D. Fuchs, V. V. Dobrovitski, D. M. Toyli, F. J. Heremans, and D. D. Awschalom, *Science* **326**, 1520 (2009).
- <sup>16</sup>A. Laucht, S. Simmons, R. Kalra, G. Tosi, J. P. Dehollain, J. T. Muhonen, S. Freer, F. E. Hudson, K. M. Itoh, D. N. Jamieson, *et al.*, *Phys. Rev. B* **94**, 161302 (2016).
- <sup>17</sup>K. R. K. Rao and D. Suter, *Phys. Rev. A* **95**, 053804 (2017).
- <sup>18</sup>P. Forn-Díaz, J. Lisenfeld, D. Marcos, J. J. García-Ripoll, E. Solano, C. J. P. M. Harmans, and J. E. Mooij, *Phys. Rev. Lett.* **105**, 237001 (2010).
- <sup>19</sup>J. Tuorila, M. Silveri, M. Sillanpää, E. Thuneberg, Y. Makhlin, and P. Hakonen, *Phys. Rev. Lett.* **105**, 257003 (2010).
- <sup>20</sup>C. Deng, J. L. Orgiazzi, F. Shen, S. Ashhab, and A. Lupascu, *Phys. Rev. Lett.* **115**, 133601 (2015).
- <sup>21</sup>T. Niemczyk, F. Deppe, H. Huebl, E. P. Menzel, F. Hocke, M. J. Schwarz, J. J. García-Ripoll, D. Zueco, T. Hümmer, E. Solano, *et al.*, *Nat. Phys.* **6**, 772 (2010).
- <sup>22</sup>A. Fedorov, A. K. Feofanov, P. Macha, P. Forn-Díaz, C. J. P. M. Harmans, and J. E. Mooij, *Phys. Rev. Lett.* **105**, 060503 (2010).
- <sup>23</sup>Y. Todorov, A. M. Andrews, R. Colombelli, S. De Liberato, C. Ciuti, P. Klang, G. Strasser, and C. Sirtori, *Phys. Rev. Lett.* **105**, 196402 (2010).
- <sup>24</sup>A. A. Anappara, S. De Liberato, A. Tredicucci, C. Ciuti, G. Biasiol, L. Sorba, and F. Beltram, *Phys. Rev. B* **79**, 201303 (2009).
- <sup>25</sup>F. Yoshihara, T. Fuse, S. Ashhab, K. Kakuyanagi, S. Saito, and K. Semba, *Phys. Rev. A* **95**, 053824 (2017).
- <sup>26</sup>J. Casanova, G. Romero, I. Lizuain, J. J. García-Ripoll, and E. Solano, *Phys. Rev. Lett.* **105**, 263603 (2010).
- <sup>27</sup>D. Ballester, G. Romero, J. J. García-Ripoll, F. Deppe, and E. Solano, *Phys. Rev. X* **2**, 021007 (2012).
- <sup>28</sup>A. L. Grimsmo and S. Parkins, *Phys. Rev. A* **87**, 033814 (2013).
- <sup>29</sup>J. S. Pedernales, I. Lizuain, S. Felicetti, G. Romero, L. Lamata, and E. Solano, *Sci. Rep.* **5**, 15472 (2015).
- <sup>30</sup>N. K. Langford, R. Sagastizabal, M. Kounalakis, C. Dickel, A. Bruno, F. Luthi, D. J. Thoen, A. Endo, and L. DiCarlo, arXiv preprint arXiv:1610.10065 (2016).
- <sup>31</sup>S. Fedortchenko, S. Felicetti, D. Marković, S. Jezouin, A. Keller, T. Coudreau, B. Huard, and P. Milman, *Phys. Rev. A* **95**, 042313 (2017).
- <sup>32</sup>R. Puebla, M. J. Hwang, J. Casanova, and M. B. Plenio, *Phys. Rev. A* **95**, 063844 (2017).
- <sup>33</sup>J. Braumüller, M. Marthaler, A. Schneider, A. Stehli, H. Rotzinger, M. Weides, and A. V. Ustinov, arXiv preprint arXiv: 1611.8404 (2016).
- <sup>34</sup>Z. Lü, Y. Yan, H. S. Goan, and H. Zheng, *Phys. Rev. A* **93**, 033803 (2016).
- <sup>35</sup>W. D. Oliver, Y. Yu, J. C. Lee, K. K. Berggren, L. S. Levitov, and T. P. Orlando, *Science* **310**, 1653 (2005).
- <sup>36</sup>S. Ashhab, J. R. Johansson, A. M. Zagoskin, and F. Nori, *Phys. Rev. A* **75**, 063414 (2007).
- <sup>37</sup>M. D. Reed, L. DiCarlo, B. R. Johnson, L. Sun, D. I. Schuster, L. Frunzio, and R. J. Schoelkopf, *Phys. Rev. Lett.* **105**, 173601 (2010).
- <sup>38</sup>P. London, P. Balasubramanian, B. Naydenov, L. P. McGuinness, and F. Jelezko, *Phys. Rev. A* **90**, 012302 (2014).